Holz Roh Werkst (2004) 62:335–342
DOI 10.1007/s00107-004-0482-1

ORIGINALARBEITEN · ORIGINALS

W. Sonderegger · P. Niemz

The influence of compression failure on the bending, impact bending and tensile strength of spruce wood and the evaluation of non-destructive methods for early detection

Published online: 29 May 2004

Abstract Bending strength (MOR) and bending Young's modulus (MOE) according to DIN 52186 and MOE calculated on the basis of eigenfrequency and sound velocity were tested on small clear wood specimens of Norway spruce wood with and without compression failure. One group of specimens was climatised in a normal climate of 20°C and 65% relative humidity, while the other group was stored for one month under water before testing. The MOR of specimens with compression failure decreased about 20% on average (normal climate and wet) compared with the specimens without compression failure. The MOE of the specimens with compression failure was reduced only minimally compared with the specimens without compression failure stored in a normal climate, but very distinct differences (more then 30%) were found under wet conditions. The MOE of the specimens with compression failure calculated on the basis of eigenfrequency and sound velocity were not reduced or only minimally compared with the specimens without compression failure. It is therefore not possible to detect compression failure and to determine reduction in MOR using eigenfrequency or sound velocity. In addition, impact bending (DIN 52189), tensile strength and tensile MOE (DIN 52188) were tested on small clear wood specimens of Norway spruce wood with and without compression failure. The specimens with compression failure revealed an average reduction in impact strength of about 40% and an average reduction in tensile strength of about 20% compared with the specimens without compression failure, whereas tensile MOE of the specimens with compression failure was not reduced compared with the specimens without compression failure. The detection of compression failure by computer tomography (CT) was tested on Norway spruce wood boards 10 cm in thickness, and detection by optical scanner was tested on planed Norway spruce wood boards. CT recognised large compression failures easily, whereas the scanner was not able to detect them.

W. Sonderegger · P. Niemz (✉)
Chair of Wood Science,
Swiss Federal Institute of Technology (ETH),
Rämistrasse 101, 8092 Zurich, Switzerland
e-mail: niemz@fowi.ethz.ch

Einfluss von Stauchbrüchen auf die Biegefestigkeit, die Zugfestigkeit und die Bruchschlagarbeit von Fichtenholz und Bewertung zerstörungsfreier Methoden zu deren Früherkennung

Zusammenfassung Es wurden die Biegefestigkeit und der Biege-E-Modul nach DIN 52186 und die Biege-E-Moduln errechnet aus Eigenfrequenz und Schallgeschwindigkeit an kleinen Fichtenproben mit und ohne Winddruckstauchungen untersucht. Ein Teil der Proben wurde vor der Prüfung bei Normalklima (20°C/65% relative Luftfeuchte) konditioniert, der andere Teil nach der Konditionierung bei Normalklima einen Monat in Wasser gelegt und danach geprüft. Bei den Proben mit Stauchungen war die Festigkeit gegenüber den Proben ohne Stauchungen sowohl bei den normalklimatisierten als auch bei den wassergelagerten Proben um mehr als 20% reduziert. Der E-Modul nach DIN war bei den normalklimatisierten Proben durch die Stauchungen nur wenig reduziert, bei den wassergelagerten Proben jedoch um mehr als 30%. Die aus der Eigenfrequenz und der Schallgeschwindigkeit errechneten E-Moduln zeigten dagegen nur eine geringe bzw. keine stauchungsbedingte Reduktion. Es war deshalb nicht möglich, mittels der zerstörungsfreien Prüfmethoden Eigenfrequenz und Ultraschall die durch die Stauchungen bedingte Festigkeitsreduktion der Proben zu erfassen. Weiter wurden die Bruchschlagarbeit nach DIN 52189 sowie die Zugfestigkeit und der Zug-E-Modul nach DIN 52188 an kleinen Fichtenproben mit und ohne Winddruckstauchungen untersucht. Bei den Proben mit Stauchungen war die Bruchschlagarbeit gegenüber den Proben ohne Stauchungen um 40–50% reduziert und die Zugfestigkeit um mehr als 20%, während der Zug-E-Modul keine Reduktion aufwies. Ferner wurde die Erkennung von Winddruckstauchungen mittels Röntgen-Computertomographie und optischem Scanner getestet. Breite Stauchungen können mittels Computertomographie gut erkannt werden, während mit heute üblichen Fehlererkennungspro-

grammen bei Scannern die Stauchungen nicht detektiert werden können.

1 Introduction

Storm Vivian on 27 February 1990 and storm Lothar on 26 December 1999 caused major damage in Switzerland and other countries in Europe, with many million cubic metres of wood affected by wind. This wood could either not be used for construction at all, or only to a limited extent, because of the formation of compression failure. Compression failure describes the buckling of fibres which often occurs on the lee side of the wind-exposed tree. Since the compression strength parallel to the fibre is only half the tensile strength, some parts of the lee side of the tree, where the highest compression strength is found, overload under major bending, resulting in the formation of compression failures. These failures can be very small and only visible through a microscope, or several millimetres wide already be detected with the naked eye (Fig. 14).

Previous investigations on the influence of compression failure on the strength of wood were in some cases contradictory. Trendelenburg (1940), testing clear wood specimens of spruce, stated that tensile strength and impact strength were already reduced by very small, microscopically fine compression failures, whereas compression strength and bending strength were reduced only by larger compression failures. Glos and Henrici (1993) noticed in tests of timber that bending strength was not reduced significantly, but that tensile strength was reduced by 22%. Koch (1999), in contrast, observed a 16% reduction in bending strength in tests of scantlings.

In order to obtain a clearer picture on the impact of compression failure on the strength of spruce wood, as part of a comprehensive project investigating the quality and use of storm-damaged wood, tests on small clear wood samples were carried out.

2 Material and methods

Specimens. Thirty Norway spruce trees (*Picea abies* [L.] Karst.) grown in the Federal Institute of Technology's research forest in Zurich which had been damaged by storm Lothar on 26 December 1999 were available to the project determining the wood quality. From each tree, 3 to 5 consecutive 5-metre trunk sections (128 in total) were cut to a fixed pattern. The specimens used for this particular project were taken from 10-cm-thick heart planks cut from the lower two metres of each trunk section. These heart planks ran parallel to the wind direction.

For bending, impact-bending and tensile tests, 50-cm-long blocks were cut from the heart planks. Wherever possible, one piece without compression failure and one or two pieces with macroscopically visible compression failure were cut from each heart plank, making sure that the compression failure was in the middle in each case. Then, slats were cut from the blocks at intervals of 35 mm, from both edges of the tree (each slat 31.5 mm wide; saw cut 3.5 mm). From these samples, 1 to 3 rough blanks were made (31.5×31.5×500 mm). The blanks were climatised in a normal climate of 20°C/65% RH, planed and cut down to their final size and shape (20×20×400 mm; growth rings standing), and climatised again in a normal climate.

For the tests on wet specimens (well above fibre saturation), 70 bending test specimens without compression failure and 50 bending test specimens with compression failure were put in water for one month.

The tensile test specimens were made from climatised bending test specimens by tapering them to a breadth of 8 mm in the middle and attaching two glue-on reinforcement strips at each end (cf. DIN 52188).

For the computer tomography tests, 3 specimens with obvious compression failure were cut from remaining portions of the heart planks (for size of specimens see Table 1).

For the scanner tests, 4 boards with compression failures were cut from the lee side of the heart planks.

Methods. Bending strength according to DIN 52186 of specimens stored in a normal climate (20°C/65% relative humidity) and stored under water (average moisture content 89.7%), tensile strength according to DIN 52188, and impact bending strength according to DIN 52189 were tested. In addition, a number of non-destructive methods for the early detection of compression failure and its influence on wood strength were tested, in some cases on the same specimens used for the strength tests: sound velocity and eigenfrequency were measured for the specimens subsequently used in the bending test, and in addition, sound velocity was measured for specimens subsequently used in the impact-bending test. Accordingly, the MOE was calculated on the basis of sound velocity and eigenfrequency and compared with the MOE according to DIN (Niemz (1993) for the formula used to calculate the MOE on the basis of sound velocity, and cf. Görlacher (1984) for the calculation on the basis of eigenfrequency).

In addition, the ability of computer tomography and scanner technology to detect compression failure was tested.

Tests. For the bending tests on specimens stored in a normal climate, 1112 specimens without compression failure and 241 specimens with compression failure were tested.

Table 1 Summary of CT tests
Tabelle 1 Zusammenstellung der CT-Prüfungen

Test no.	Dimensions (length ×breadth×height)	No. of tomographs	Section	Height of section (in mm from bottom of specimen)
A052	160×120×100	11	Length×breadth (radial to tangential section)	10; 20; 30; 40; 50; 60; 70; 76; 80; 90; 96
A102–1	180×150 (115[a])×100	17	Length×breadth (radial to tangential section)	10; 15; 20; 25; 30; 35; 40; 45; 50; 55; 60; 65; 70; 75; 80; 85; 90
		1	Breadth×height (cross section)	106
A102–2	180×150 (110[a])×100	1	Length×breadth (radial to tangential section)	50

[a] Upper breadth shorter owing to waney edge

One problem was the large proportion of compression wood on the lee side of the heart planks, where most compression failures were also to be found. For this reason, the results of some tests were subdivided into two categories: results for all specimens, and results for clear specimens containing a maximum of 5% compression wood (cf. Tables 2 and 5). This was done for the normal-climate bending tests and the impact bending tests wherever a sufficient number of specimens were tested making such a subdivision possible.

The impact bending test was carried out on 158 specimens without compression failure and 70 specimens with compression failure.

The tensile test was performed on 79 specimens without compression failure and 23 specimens with compression failure.

The computer tomography tests were carried out at the Centre for Non-Destructive Testing (ZZfP) at the EMPA in Dübendorf, using an X-ray computer tomograph. Given the size of the specimens, it was only possible to scan at a resolution of 0.2 mm. Table 1 contains details of the images in summary. For the first two specimens (A052 and A102-1), tomographs were taken of different layers in radial to slightly tangential section, in the case of specimen A052 at intervals of 10 mm (plus two additional tomographs at 76 and 96 mm), and in the case of specimen A102-1 at intervals of 5 mm. For the third specimen (A102-2), only one tomograph was taken, half way up the specimen. In addition, a tomograph of specimen A102-1 was taken in cross section.

Four 1200-mm-long planed boards with compression failure between 0.1 and 2.5 mm wide were scanned at Scanimation Europe, Dresden, using an industrial scanner system (ScanChop LCS-2). The tests were done with both a colour camera (Type TVI high-resolution RGB: 0.2 mm pixel width) and a black and white camera (Type IVP 2500 with 0.4 mm linewidth resolution and 0.15–0.2 mm height resolution).

3 Results

3.1 Bending test on normal climate specimens

The specimens with compression failure showed an average reduction in MOR of over 20% compared with the specimens without compression failure (Table 2). Further, the MOR was strongly dependent on the width of the compression failure (Fig. 1). While the MOR for specimens with compression failures with a width of $\leq$0.1 mm revealed an average reduction of only 10% compared with the specimens without compression failure, MOR for specimens with compression failures of 1.5 mm and more

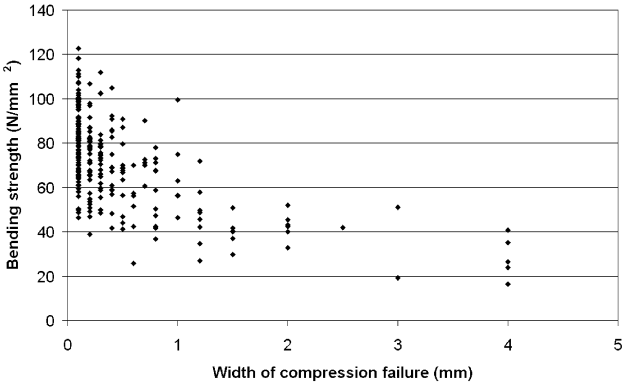

Fig. 1 Bending strength versus width of compression failure (normal climate)
Abb. 1 Einfluss der Breite der Stauchbrüche auf die Biegefestigkeit (Normalklima)

Table 2 Influence of compression failure on bending strength, MOE according to DIN and MOE calculated on the basis of eigenfrequency ($E_{b.ef}$) and sound velocity ($E_{b.sound}$) for specimens stored in a normal climate (20°C/65% RH). The means of all specimens (total) and of the specimens without compression wood (clear) are specified. Coefficient of variation in brackets. The percentages refer to the specimens without compression failure

Tabelle 2 Einfluss von Stauchbrüchen auf die Biegefestigkeit, den E-Modul, ermittelt nach DIN, und die E-Moduln, berechnet aus der Schallgeschwindigkeit ($E_{b.ef}$) und der Eigenfrequenz ($E_{b.sound}$), bei Prüfung im Normalklima (20°C/65% rel. Luftfeuchtigkeit). Mittelwerte aller geprüften Proben (total) und derjenigen ohne Druckholz (clear); Variationskoeffizient (in Klammern); Prozentzahlen, bezogen auf die Proben ohne Stauchungen

	Without compression failure		With compression failure		With compression f ailure		With compression failure	
			≤0.1 mm		>0.1 mm		All specimens	
	Total	Clear	Total	Clear	Total	Clear	Total	Clear
Number of specimens	1112	687	89	23	152	39	241	62
Density at normal climate (kg/m³)	**484** (12.80) 100%	472 (10.79) 100%	**513** (12.67) 106.0%	482 (12.07) 102.1%	**532** (10.47) 109.9%	504 (9.83) 106.8%	**525** (11.41) 108.5%	496 (10.77) 105.1%
Bending strength (N/mm²)	**90.29** (16.27) 100%	92.66 (14.95) 100%	**82.75** (19.81) 91.6%	82.79 (17.03) 89.3%	**63.94** (29.92) 70.8%	66.13 (29.02) 71.4%	**70.89** (28.62) 78.5%	72.21 (26.55) 77.9%
MOE according to DIN (N/mm²)	**13,167** (20.80) 100%	14,101 (16.25) 100%	**13,272** (20.42) 100.8%	13597 (18.26) 96.4%	**12,429** (23.87) 94.4%	13,281 (22.97) 94.2%	**12,740** (22.75) 96.8%	13,396 (21.20) 95.0%
$E_{b.ef}$ (N/mm²)	**13,282** (19.97) 100%	14,160 (15.77) 100%	**13,605** (18.65) 102.4%	13,748 (17.92) 97.0%	**13,517** (18.68) 102.2%	14,399 (17.24) 101.7%	**13,584** (18.59) 102.3%	14,161 (17.48) 100.0%
$E_{b.sound}$ (N/mm²)	**15,932** (18.51) 100%	16,609 (15.59) 100%	**17,019** (17.26) 106.8%	17,179 (17.55) 103.4%	**17,247** (15.96) 108.3%	17,680 (14.69) 106.4%	**17,163** (16.42) 107.7%	17,498 (15.68) 105.4%

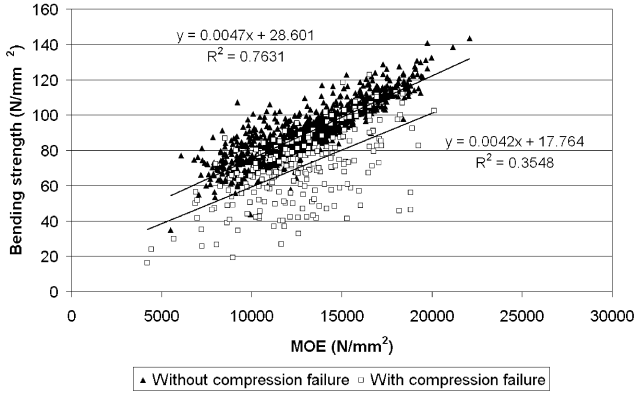

Fig. 2 Bending strength versus MOE according to DIN (normal climate)
Abb. 2 Biegefestigkeit in Korrelation zum E-Modul nach DIN (Normalklima)

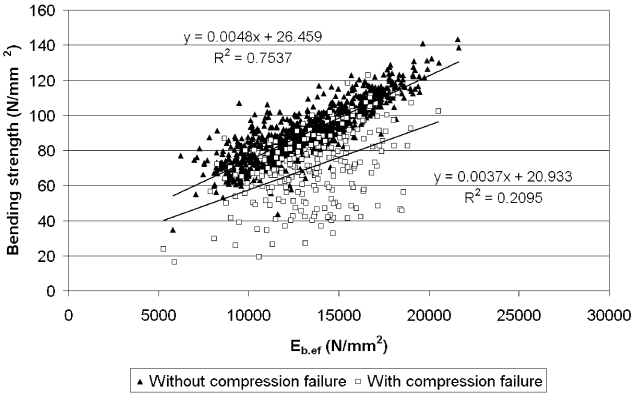

Fig. 3 Bending strength versus MOE according to $E_{b.ef}$ on normal climate
Abb. 3 Biegefestigkeit in Korrelation zum E-Modul, berechnet aus der Eigenfrequenz bei Normalklima

in width decreased about 58% to an average MOR of 37.5 N/mm^2.

The influence of compression failure on the MOE according to DIN was low. The average MOE for specimens with compression failure was reduced to only 5% compared with specimens without compression failure (Table 2). Further, the coefficient of determination between the MOR and the MOE was small (R^2=0.35) for the specimens with compression failure, whereas the specimens without compression failure had a coefficient of determination of R^2=0.76 (Fig. 2).

On the MOE calculated on the basis of non-destructive methods—eigenfrequency ($E_{b.ef}$) and sound velocity ($E_{b.sound}$)—the influence of compression failure was even lower than on the MOE according to DIN. While $E_{b.ef}$ remained more or less constant over all measurements, $E_{b.sound}$ increased slightly for the specimens with compression failure in line with their higher density. According to this the coefficient of determination between the MOR and $E_{b.ef}$ for the specimens with compression failure was very low at R^2=0.21. At R^2=0.08, there was practically no correlation at all between the MOR and $E_{b.sound}$ (Figs. 3 and 4).

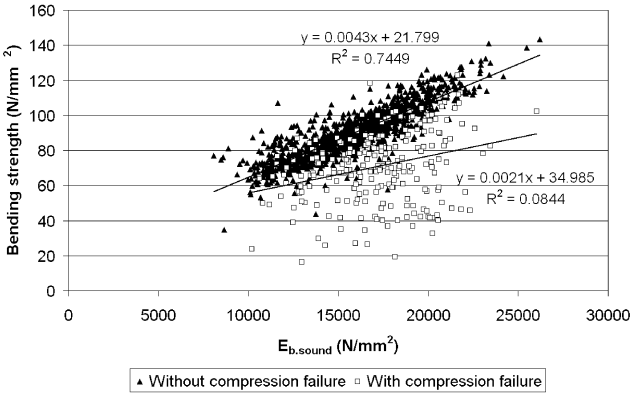

Fig. 4 Bending strength versus MOE according to $E_{b.sound}$ on normal climate
Abb. 4 Biegefestigkeit in Korrelation zum E-Modul, berechnet aus der Schallgeschwindigkeit bei Normalklima

3.2 Bending test on specimens stored in water

As expected, the MOR of specimens stored in water was much lower (more than 40% lower on average) than that of specimens stored in a normal climate (cf. Niemz 1993). However, the effect of compression failure on water-stored and normal-climate specimens was similar (Table 3), with both types of specimen losing around 20% of their strength on average. However, the reduction in the strength of water-stored specimens with wider compression failure was less pronounced than for specimens of the same width stored in a normal climate (Fig. 5). For widths of 1.5 mm and more the mean reduction in strength was 43% compared with the specimens without compression failure (normal-climate specimens 58%, see above).

The bending MOE according to DIN was significantly affected by compression failure (unlike the normal-climate specimens). This was reflected in a substantial 34% reduction in MOE for the specimens with compression failure compared with the specimens without compression failure (Table 3). Further, Fig. 6 (bending strength versus MOE according to DIN) shows only a slightly lower regression line for the specimens with compression failure. However, the coefficient of determination was low, both for specimens without compression failure (R^2=0.34) and those with compression failure (R^2=0.32).

As was the case with normal-climate specimens, MOE calculated on the basis of eigenfrequency and sound velocity displayed only minimal correlation with strength for the specimens with compression failure. While $E_{b.ef}$ decreased slightly for specimens with compression failure, $E_{b.sound}$ remained fairly constant. At R^2=0.26, the coefficient of determination for $E_{b.ef}$ was also very small, and R^2=0.04 for $E_{b.sound}$ indicates virtually no correlation with strength at all (Fig. 7, 8).

Table 3 Influence of compression failure on bending strength, MOE according to DIN and MOE calculated on the basis of eigenfrequency ($E_{b.ef}$) and sound velocity ($E_{b.sound}$) for specimens stored in water (average moisture content 89.7%). Represented are the mean and, in brackets, the coefficient of variation. The percentages refer to the specimens without compression failure

Tabelle 3 Einfluss von Stauchbrüchen auf die Biegefestigkeit, den E-Modul, ermittelt nach DIN, und die E-Moduln, berechnet aus der Schallgeschwindigkeit ($E_{b.ef}$) und der Eigenfrequenz ($E_{b.sound}$), bei Prüfung nach Wasserlagerung der Proben (mittlere Holzfeuchte 89,7%). Mittelwerte; Variationskoeffizient (in Klammern); Prozentzahlen, bezogen auf die Proben ohne Stauchungen

	Without compression failure	With compression failure	With compression failure	With compression failure
		≤0.1 mm	>0.1 mm	All specimens
Number of specimens	70	14	36	50
Density at normal climate	**488**	**477**	**510**	**501**
20°C/65% RH (kg/m^3)	(9.35)	(11.16)	(10.46)	(10.97)
	100%	97.7%	104.5%	102.7%
Bending strength (N/mm^2)	**52.36**	**45.92**	**39.97**	**41.63**
	(12.61)	(16.02)	(25.28)	(23.36)
	100%	87.7%	76.3%	79.5%
MOE according to DIN (N/mm^2)	**12,266**	**8,099**	**8,163**	**8,145**
	(15.74)	(11.38)	(30.59)	(26.56)
	100%	66.0%	66.5%	66.4%
$E_{b.ef}$ (N/mm^2)	**10,782**	**9,711**	**10,404**	**10,210**
	(14.65)	(11.58)	(15.98)	(15.20)
	100%	90.1%	96.5%	94.7%
$E_{b.sound}$ (N/mm^2)	**19,927**	**18,752**	**20,684**	**20,143**
	(12.74)	(8.73)	(10.37)	(10.84)
	100%	94.1%	103.8%	101.1%

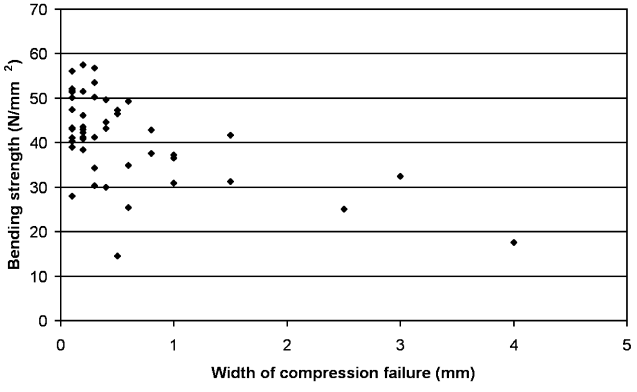

Fig. 5 Bending strength versus width of compression failure (water stored)
Abb. 5 Einfluss der Breite der Stauchbrüche auf die Biegefestigkeit (wassergelagerte Proben)

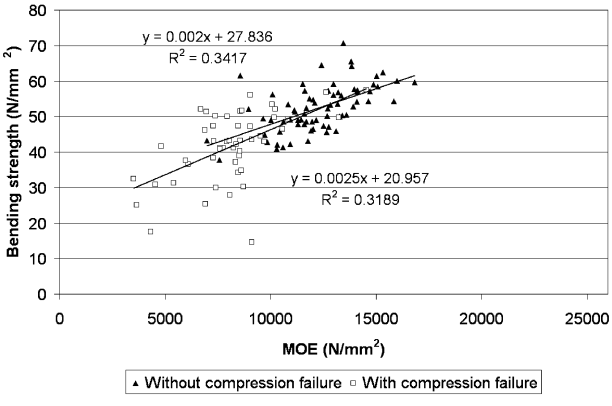

Fig. 6 Bending strength versus MOE according to DIN (water stored)
Abb. 6 Biegefestigkeit in Korrelation zum E-Modul nach DIN (wassergelagerte Proben)

3.3 Tensile test

The tensile strength of the specimens with compression failure was around 23% lower than for those without compression failure. The tensile MOE according to DIN displayed no influence to compression failure, but increased with higher density and decreased with lower density (Table 4). This is also reflected in Fig. 9 in the lower coefficient of determination between tensile strength and MOE for the specimens with compression failure (R^2=0.35) than for specimens without compression failure (R^2=0.53).

3.4 Impact-bending test

In Table 5, if all specimens tested are compared, the impact bending of specimens with compression failure is around 40% lower than for those without compression failure. The difference is even higher for clear specimens (almost 47%). The reduction is already around 40% for specimens with compression failure of a width of 0.1 mm or less, and not much more for wider compression failure. Comparing impact-bending strength with the MOE calculated on the basis of sound velocity gives only a low correlation (R^2=0.33 for specimens without compression failure, R^2=0.15 for those with compression failure; cf. Fig. 10).

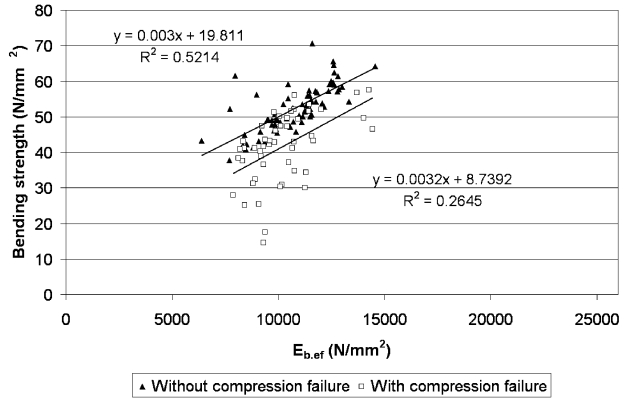

Fig. 7 Bending strength versus MOE according to $E_{b.ef}$ on specimens stored in water
Abb. 7 Biegefestigkeit in Korrelation zum E-Modul, berechnet aus der Eigenfrequenz bei den wassergelagerten Proben

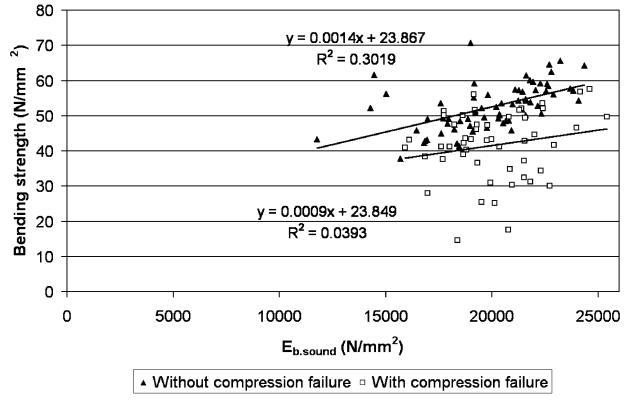

Fig. 8 Bending strength versus MOE according to $E_{b.sound}$ on specimens stored in water
Abb. 8 Biegefestigkeit in Korrelation zum E-Modul, berechnet aus der Schallgeschwindigkeit bei den wassergelagerten Proben

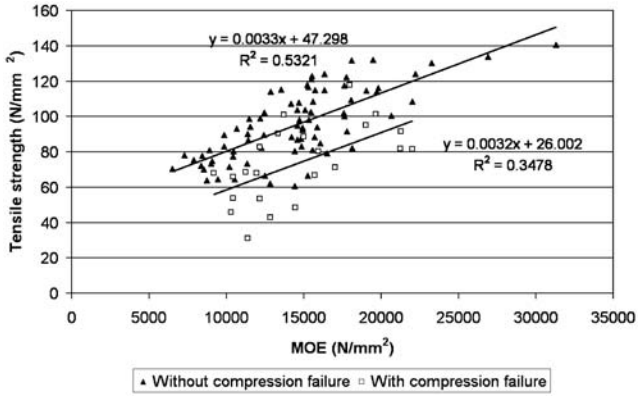

Fig. 9 Tensile strength versus tensile MOE
Abb. 9 Korrelation zwischen Zugfestigkeit in Faserrichtung und Zug-E-Modul

3.5 Computer tomography test

Compression failure showed up as light-coloured lines (longitudinal section) and light-coloured bands (cross-section) on computer tomographs (Figs. 11, 12, 13, cf. Fig. 14). Due to the low resolution of the images (pixel width 0.2 mm), fine cracks were not visible. However, computer tomography allows the inside of the wood specimen to be examined. In the case of specimen A102-2, where compression failure was visible superficially on only one side, a single computer tomograph taken half way up the specimen showed that the compression failure extended at least half way through the specimen.

Specimen A052 shows the influence of a branch on the formation of compression failure (cf. Figs. 11 and 12). On the computer tomographs the compression failure disappears close to the branch. The length and breadth of the reaction wood also decrease close to the branch. Since, however, the reaction wood does not disappear completely, it can be assumed that there is also compression failure close to the branch, not visible in images of this resolution. In Fig. 11 the reaction wood resulting from

Table 4 Influence of compression failure on tensile strength and tensile MOE of specimens stored in a normal climate (20°C/65% RH). Represented are the mean and, in brackets, the coefficient of variation. The percentages refer to the specimens without compression failure

Tabelle 4 Einfluss der Stauchbrüche auf die Zugfestigkeit in Faserrichtung und den Zug-E-Modul bei Prüfung im Normalklima (20°C/65% rel. Luftfeuchtigkeit). Mittelwerte; Variationskoeffizient (in Klammern); Prozentzahlen, bezogen auf die Proben ohne Stauchungen

	Without compression failure	With compression failure	With compression failure	With compression failure
		≤0.1 mm	>0.1 mm	All specimens
Number of specimens	79	13	10	23
Density at normal climate (kg/m³)	**451**	**424**	**476**	**447**
	(12.23)	(11.70)	(11.82)	(12.92)
	100%	94.0%	105.5%	99.1%
Tensile strength (N/mm²)	**95.22**	**76.75**	**69.64**	**73.66**
	(20.88)	(25.46)	(34.86)	(29.19)
	100%	80.6%	73.1%	77.4%
MOE according to DIN (N/mm²)	**14,514**	**13,423**	**16,412**	**14,723**
	(30.27)	(25.10)	(24.95)	(26.61)
	100%	92.5%	113.1%	101.4%

Table 5 Influence of compression failure on impact strength and MOE calculated on the basis of sound velocity ($E_{i.sound}$) for specimens stored in a normal climate (20°C/65% RF). The means of all specimens (total) and of the specimens without compression wood (clear) are specified. Coefficient of variation in brackets. The percentages refer to the specimens without compression failure

Tabelle 5 Einfluss der Stauchbrüche auf die Bruchschlagarbeit und den E-Modul, berechnet aus der Schallgeschwindigkeit, bei Prüfung im Normalklima (20°C/65% rel. Luftfeuchtigkeit). Mittelwerte aller geprüften Proben (total) und derjenigen ohne Druckholz (clear); Variationskoeffizient (in Klammern); Prozentzahlen, bezogen auf die Proben ohne Stauchungen

	Without compression failure		With compression failure ≤0.1 mm		With compression failure >0.1 mm		With compression failure All specimens	
	Total	Clear	Total	Clear	Total	Clear	Total	Clear
Number of specimens	158	91	36	8	34	8	70	16
Density at normal climate (kg/m³)	**499** (12.15) 100%	484 (11.38) 100%	**499** (12.59) 100%	491 (11.14) 101.4%	**538** (13.94) 107.8%	480 (11.67) 99.2%	**518** (13.76) 103.8%	485 (11.09) 100.2%
Impact strength (kJ/m²)	**43.05** (37.21) 100%	50.87 (29.49) 100%	**26.30** (32.75) 61.1%	29.96 (44.38) 58.9%	**25.58** (35.23) 59.4%	24.22 (11.36) 47.6%	**25.95** (33.73) 60.3%	27.09 (35.95) 53.3%
$E_{i.sound}$ (N/mm²)	**16,324** (18.58) 100%	**17,428** (15.62) 100%	**16,720** (16.99) 102.4%	**18,084** (14.08) 103.8%	**18,109** (16.55) 110.9%	**17,492** (13.48) 100.4%	**17,395** (17.13) 106.6%	17,788 (13.44) 102.1%

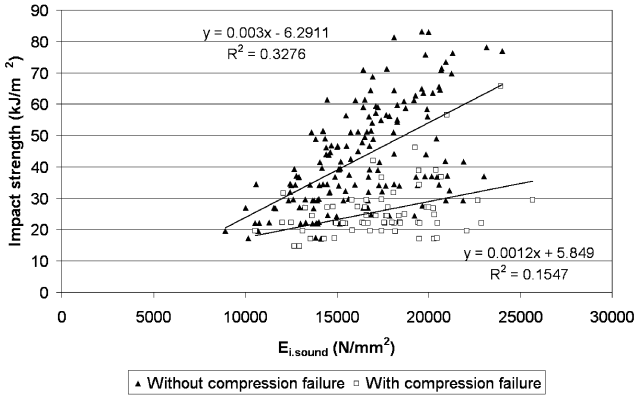

Fig. 10 Impact strength versus MOE on the basis of sound velocity ($E_{i.sound}$)
Abb. 10 Korrelation zwischen der Bruchschlagarbeit und dem E-Modul, berechnet aus der Schallgeschwindigkeit

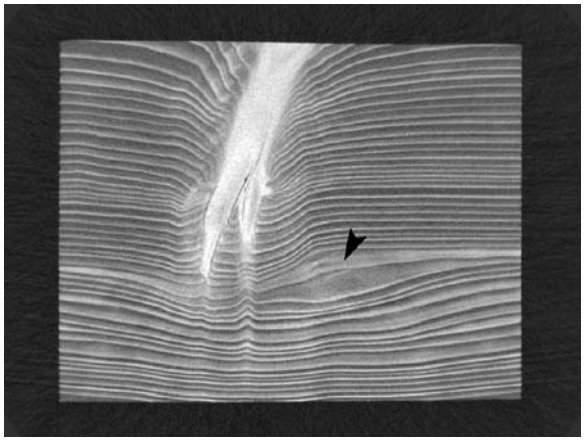

Fig. 11 Computer tomographic images: longitudinal sections through specimen A052 at heights of 30 mm
Abb. 11 Computertomographische Aufnahmen von Stauchbrüchen: Längsschnitt durch Probe AO52 in einer Höhe von 30 mm

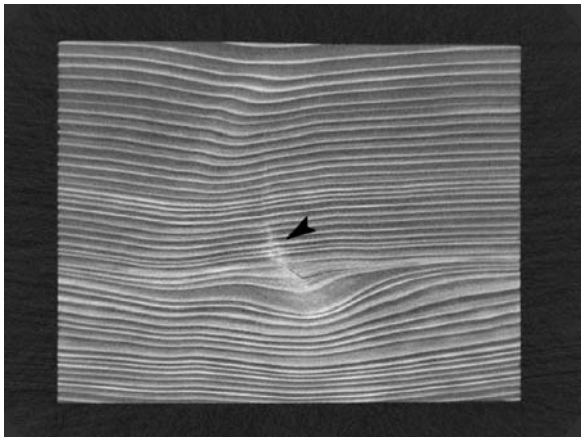

Fig. 12 Computer tomographic images: longitudinal sections through specimen A052 at heights of 70 mm
Abb. 12 Computertomographische Aufnahmen von Stauchbrüchen: Längsschnitt durch Probe AO52 in einer Höhe von 70 mm

compression failure is clearly visible right of the branch, but the compression failure itself is no longer visible. As one moves further from the branch, where the fibres are deflected less from the longitudinal, the compression failure is clearly visible once again (Fig. 12).

In the case of specimen A102-1 the compression failure can be easily traced through all sections. All the computer tomographs show continuous compression failure.

3.6 Scanner test

Neither the black and white nor the colour camera were able to record compression failure adequately to produce data sets which could be evaluated to detect compression failure. This is due on the one hand to the low resolution (0.15–0.4 mm pixel width), which allowed only wider instances of compression failure to be recorded. Another important factor is that in scanner images, the colours or grey tones representing compression failure are not suf-

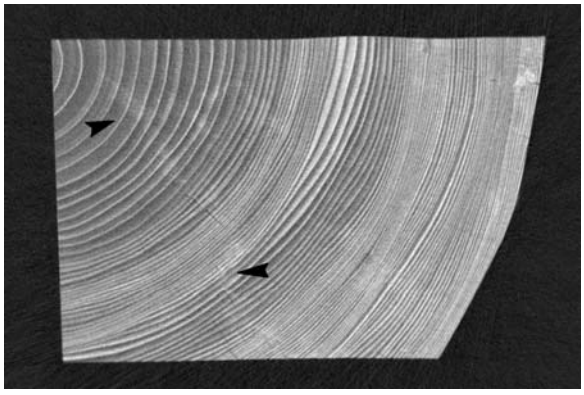

Fig. 13 Computer tomographic images: cross-section through specimen A102-1 at a height of 106 mm
Abb. 13 Computertomographische Aufnahmen von Stauchbrüchen: Querschnitt durch Probe A102-1 in 106 mm Höhe

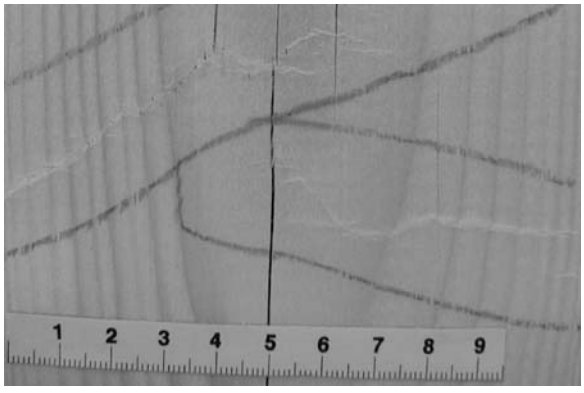

Fig. 14 Compression failure (digital camera)
Abb. 14 Foto eines Stauchbruches mit Digitalkamera

ficiently different from the colours and tones representing clear wood to generate adequate data for evaluation.

4 Discussion

Compared to all the types of strength investigated, impact-bending strength is the most strongly affected by compression failure, with a mean reduction in strength of between 40% and 47%. This tallies with the findings of Koch (1999), who even observed a mean reduction in strength of over 60%, albeit on fibre-saturated specimens (cf. also Koch 1996).

Impact-bending strength and tensile strength decrease sharply even with compression failure of a width of 0.1 mm or less (around 40% and 20% respectively), and in both cases the reduction in strength is not much more pronounced for compression failure of more than 0.1 mm. However, bending strength decreases only minimally, between 8% and 12%, for compression failure less than or equal to 0.1 mm wide, but decreases around 60% when there is wide compression failure (cf. Fig. 1). This tallies with the observations of Trendelenburg (1940), who detected a clear reduction in impact-bending strength and tensile strength, but not in bending strength, even with compression failure of microscopic width.

Unlike Glos and Henrici (1993) testing timber, the present investigation of clear wood specimens observed a sharp decline in the bending strength (around 20% on average) of specimens with compression failure stored both in a normal climate and in water.

According to Glos and Henrici (1993) and Koch (1999), no significant reduction in MOE according to DIN was observed in bending tests (normal climate) or tensile strength tests for specimens with compression failure. One exception were bending test specimens stored in water, where MOE decreased even more than MOR. It is interesting that there is a substantial reduction in MOE even in cases where only fine compression failure occur. Trendelenburg (1940) also observed a significant reduction in the bending MOE of specimens with compression failure. However, the data give no indication of whether the specimens were tested in a fibre-saturated or normal-climate state.

As far as using non-destructive methods—eigenfrequency and sound velocity—to assess the strength of specimens with compression failure is concerned, bending tests and impact-bending tests (sound velocity only) demonstrated only a minimal correlation, or no correlation at all, between the MOE calculated on the basis of eigenfrequency and sound velocity and the bending or impact-bending strength. This shows that detecting compression failure and its influence on bending and impact-bending strength is not possible using the two non-destructive methods investigated, eigenfrequency and sound velocity.

The ability of CT and scanner technology to detect compression failure is strongly dependent on the resolution of the equipment used. The higher the resolution, the finer the compression failure that can be detected. Using CT it is possible to see the extent of compression failure inside a specimen. However, with the error-detection programs currently available, automatic detection using a scanner is not possible for industrial purposes.

References

Glos P, Henrici D (1993) Festigkeitseigenschaften von Bauschnittholz aus Fichtensturmholz. Abschlussbericht 90504/5 an die Bayerische Forstliche Versuchs- und Forschungsanstalt (FVA) über das Projekt "X 17"

Görlacher R (1984) Ein neues Messverfahren zur Bestimmung des Elastizitätsmoduls von Holz. Holz Roh- Werkstoff 42:219–222

Koch G (1999) Sekundäre Veränderungen im Holz dynamisch beanspruchter Fichten (*Picea abies* [L.] Karst.) aus immissionsbelasteten und windexponierten Hochlagenbeständen. Mitteilungen der Bundesforschungsanstalt für Forst- und Holzwirtschaft, Hamburg, Nr. 192

Koch G, Schwab E, Kruse K, Bauch J (1996) Untersuchung der dynamischen Belastbarkeit des Holzes sekundär geschädigter Fichten (*Picea abies* [L.] Karst.) aus extrem windexponierten Hochlagen des Osterzgebirges. Holz Roh- Werkstoff 54:313–319

Niemz P (1993) Physik des Holzes und der Holzwerkstoffe. DRW-Verlag, Leinfelden-Echterdingen

Trendelenburg R (1940) Über Faserstauchungen in Holz und ihre Überwallung durch den Baum. Holz Roh- Werkstoff 3:209–221